Optimized Trifluoromethylation and OH Radical Labeling with Radiolysis Provide Two Fold Enhancement in the Resolution of Hydroxyl Radical Protein Footprinting

Rohit Jain[1,2,3], Erik R. Farquhar[1,3], Nanak S. Dhillon[3], † Nayeon Jeon[3], Mark R. Chance[1,2,3], Janna Kiselar[2,3*]

[1]Center for Synchrotron Biosciences, Case Western Reserve University, School of Medicine, 10900 Euclid Avenue, Cleveland, Ohio 44106, USA; [2]Center for Proteomics and Bioinformatics, Case Western Reserve University, School of Medicine, 10900 Euclid Avenue, Cleveland, Ohio 44106, USA; [3]Department of Nutrition, Case Western Reserve University, School of Medicine, 10900 Euclid Avenue, Cleveland, Ohio 44106, USA.

ABSTRACT: Hydroxyl radical based protein footprinting (HRPF) coupled with mass spectrometry is a valuable medium-resolution technique in structural biology, facilitating the assessment of protein structure and molecular-level interactions in a wide range of solution conditions. In hydroxyl radical protein footprinting with X-rays (XFP), hydroxyl radicals (•OH) generated by water radiolysis covalently label multiple amino acid (AA) side chains simultaneously. However, HRPF technologies faces challenges in achieving their full potential due to the broad (>10^3) dynamic range of AA's reactivity to •OH and the difficulty to detect slightly modified residues, particularly in peptides with highly reactive residues like methionine-containing peptides and in peptides containing all low reactive residues. To overcome this limitation, we developed a synchrotron-based multiplex labeling chemistry that utilizes CF_3 radicals (•CF_3) produced from a trifluoromethylation (TFM) reagent under controlled and optimized •OH doses generated by X-rays. We optimized the dual •CF_3/•OH chemistry in this TFM labeling approach using six model peptides and lysozyme, thereby extending the existing •OH labeling platform with simultaneous •CF_3 labeling. This optimization led to a two-fold increase in labeled AAs in multiplex TFM labeling, primarily by labeling to a greater degree AAs with low •OH reactivity via the •CF3 channel, while moderate and highly •OH reactive AAs were labeled in both •CF3 and •OH channels. Importantly, the low reactivity of methionine to •CF_3 enabled the detection and quantification of additional AAs labeled by •CF_3 across methionine-containing peptides. Consistent with observations in model peptides and protein, we observed a balanced dual •CF_3/•OH chemistry and more uniform labeling of residues in both •CF_3/•OH channels optimizing protein footprinting. Furthermore, the solvent accessibility of lysozyme residues directly correlated with •CF_3 labeling demonstrating that multiplex labeling enables a high-resolution assessment of molecular interactions for enhanced HRPF.

INTRODUCTION

Protein footprinting with mass spectrometry (PF-MS), comprising techniques like hydrogen-deuterium exchange (HDX) and hydroxyl radical protein footprinting (HRPF) are utilized in structural biology to assess macromolecular structure, macromolecular recognition, and dynamics.[1-4] X-ray footprinting of macromolecules (XFP) employs hydroxyl radicals (•OH) generated via water radiolysis to probe solvent-accessible surfaces of macromolecules and their complexes, demonstrating applications across diverse protein and nucleic acid systems.[5-7] XFP is a highly valuable tool in structural biology due to the wide and facile reactivity of •OH, which possesses van der Waals surface area and solvent properties akin to water molecules probing the same surface areas.[8] When coupled with mass spectrometry (MS), XFP offers insights into solvent accessibility and amino acid (AA) reactivity through irreversible chemical modifications, effectively correlating AA's oxidation with solvent exposure and aiding protein structural characterization.[7, 9]

Despite their utility, XFP and HRPF methods in general encounter challenges in achieving their full potential resolution (e.g. most or all residues labeled within every peptide) stemming from the broad (>10^3) dynamic range of AA reactivity to •OH, with routine easily detectible modifications occurring predominantly on a subset of AAs due to their higher reactivity, while lower reactive AAs are less frequently detected as oxidized or detected with lower signal to noise, rendering the structural information questionable. Specifically, the side chains with the lowest •OH reactivity (Thr < Ser < Pro < Glu < Asn < Asp < Ala < Gly) are typically less frequently detected as oxidized relative to much more reactive sulfur-containing and aromatic amino acids (Met < Trp < Tyr < Phe < His), while aliphatic amino acids (Leu < Ile < Arg < Val) lie in between these extremes. Methionine (Met) presents a particular challenge due to its high reactivity and background oxidation, potentially overshadowing modifications in Met-containing sequences.[10-11]

Overall, low labeling propensity of AAs with low reactivity to •OH and the high labeling propensity of Met residue diminishes XFP reactivity coverage to only 5-20% of residues within each peptide and thus overall in the structure.[11] To address these limitations, various strategies have been explored, including the incorporation of multiple complementary covalent labeling techniques like carboxyl group footprinting for labeling aspartic acid and glutamic acid residues.[12] However, these strategies often target specific AAs and may not adequately capture protein conformational changes.[13] Other novel reagents such as the use of trifluoromethylation (TFM, •CF3) mediated by •OH from a TFM reagent, offers a rapid and broad chemical labeling reactions.[13] This "combination shot" approach offers broad residue coverage, with •CF_3 labeling (+68 Da) detected on 18 out of 20 AAs, including those with "low reactivity" to •OH. TFM labeling on large biomolecules such as beta-lactoglobulin, myoglobin, and vitamin K epoxide reductase using radiolytic and photolytic labeling approaches has demonstrated its potential in structural biology.[13-15] Subsequent comparison of apo/holo-myoglobin footprints using radiolytic labeling revealed that TFM labeling is sensitive to changes in protein conformation and solvent accessibility. Independent exposure of myoglobin to TFM and HRPF demonstrated the complementarity of both techniques in increasing reactivity coverage.[14] However, TFM labeling yielded fewer additional AAs (9 / 153) than HRPF in this complementary approach. Consequently, consolidating •CF_3 and •OH footprints from independent experiments does not offer comprehensive results for protein footprinting studies and requires twice the effort.

The multiplex approach, capable of simultaneously directing both •CF_3 and •OH towards labeling AAs in a "one-pot synthesis," has shown promise for significantly advancing HRPF as an accessible high-resolution structural biology technique.[11] In this study, multiplex TFM labeling was demonstrated to label all 20 AAs with either or both •CF_3 and •OH in a "one-pot synthesis". Water radiolysis with X-ray exposure on millisecond timescale were used to release •CF_3 from a water-soluble TFM reagent (sodium triflinate, CF_3SO_2Na). However, implementing multiplex TFM labeling for protein footprinting presents challenges. Firstly, the reactivity of •CF3/•OH for 20 AAs in multiplex TFM labeling was assessed in a competition-free environment, which may differ in the protein environment. Secondly, synchrotron-based multiplex labeling chemistry relies on producing •CF_3 from a trifluoromethylation (TFM) reagent using micromolar •OH concentrations generated via X-rays, and where •OH can be continuously produced in micromolar concentrations with fluxes and timescales under beamline control.[11, 14] Our interpretation of the reactions involved suggests that transfer of radicals from •OH to CF_3SO_2Na, forming •CF_3 is enabled by sustained availability of •OH radicals over 10s of milliseconds.[13] However, a balance of radical chemistry is crucial for optimizing both •CF_3 and •OH labeling for comprehensive footprinting coverage.

To ensure the success of a multiplex TFM (dual •CF_3/•OH chemistry) protein footprinting experiment, CF_3SO_2Na concentrations and absorbed •OH amount were carefully selected to ensure optimal multiplex labeling of residues with •CF_3 and •OH modifications. We conducted a comprehensive assessment of the chemistry of •OH induced multiplex TFM labeling using six model peptides, each having specifically selected and diverse amino acid (AA) compositions. Sodium triflinate (CF_3SO_2Na) was utilized as the TFM labeling reagent, and synchrotron X-rays from the 17-BM beamline at NSLS-II were used for radiolysis-based generation of •OH. The baseline dataset from model peptides was employed to evaluate the robustness of multiplex TFM labeling, which was then applied to hen egg white lysozyme (129 AAs, 14.3 kDa). Additionally, we investigated whether both •CF_3 and •OH labels in lysozyme are consistent with protein structure and solvent-accessibility, which are essential requirements for successful protein footprinting. Overall, we have optimized conditions for multiplex labeling chemistry that increases the number of labeled probes by ~two-fold resulting in most or all of solvent accessible residues labeled within each peptide and thus overall in the structure, while balancing dynamic range of labeling within 10 folds and providing more uniform modification of residues in •CF_3/•OH channels for six model peptides and the protein lysozyme. The presented multiplex labeling technology for model peptides and protein represents a major advance in HRPF making it an accessible and high-resolution structural biology technique.

RESULTS AND DISCUSSION

Optimization of multiplex TFM chemistry using model peptides. The model peptides selected for this study were chosen based on their AA composition resembling peptide sequences commonly observed in digested protein sequences. These peptides are arranged according to the •OH reactivity of their AAs, as shown in Table 1. For example, BACHEM Synthetic (Syn) peptide contained all low •OH reactive AAs; [Glu1]-Fibrinopeptide (Glu-Fib) consisted mostly of low •OH reactive AAs with the exception of two medium •OH reactive Phe AAs (F10 and F11); Angiotensin II (AG-II) contained a mixture of low and medium •OH reactive AAs while Fibrinopeptide (FAP), [Met5]-Enkephalin (Met5) and Amyloid β-protein fragment 35-25 (Amyl-B) peptides contained multiple highly •OH reactive AAs such as Trp and Met.

We first optimized the dual •CF_3/•OH chemistry for these model peptides by initially testing various CF_3SO_2Na concentrations while maintaining a fixed absorbed •OH amount (32.2×10^{15}) at the 17-BM X-ray footprinting beamline. Specifically, we exposed all model peptides (20 µM) independently for 20 ms of X-ray beam, using a fixed aluminum (Al) attenuation of 76 µm thickness. CF_3SO_2Na concentrations ranged from 0.25 mM to 30 mM, and the extent of •CF_3 and •OH modifications for each peptide was quantified using nanoLC-MS/MS. The extent of •CF_3 and •OH labeling varied as a function of CF_3SO_2Na concentration (0.25 - 30 mM) for all six peptides (Figure 1). Notably, at the lowest CF_3SO_2Na concentration (0.25 mM), there was a significant reduction in unmodified peptide due to peptide degradation/cleavage. Peptide cleavage/degradation was moderately observed at 0.75 mM CF_3SO_2Na, and we determined that 2.5 - 30 mM of CF_3SO_2Na was ideal for quantifying the unmodified product in peptide TFM footprinting experiments without overexposing the sample. Moreover, 30 mM of CF_3SO_2Na exhibited a significant scavenging effect for both •CF_3 and •OH labeling chemistries for all peptides except the

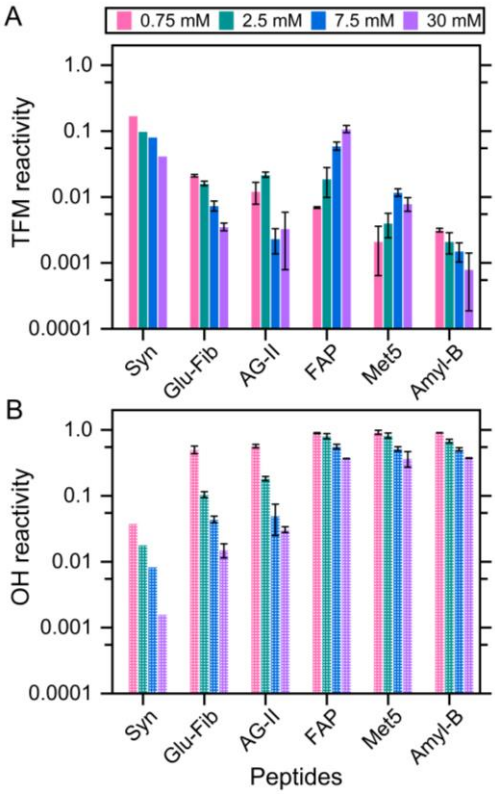

Figure 1. The dual •CF_3/•OH chemistry in multiplex TFM labeling was optimized with six model peptides by varying sodium triflinate (CF_3SO_2Na) concentration and keeping a constant number of absorbed •OH radicals (32.2×10^{15}). The average modified fraction of (A) •CF_3 (solid bars) and (B) •OH (checkered bars) was plotted on Log_{10} scale for 6 model peptides at different TFM reagent concentrations (magenta, green, blue and purple). Individual peptides with different CF_3SO_2Na concentrations were irradiated with X-rays for 20 ms at 76 µm Al thickness attenuation on 17-BM beamline, NSLS-II. Experiments were done in two replicates and error bars represents their standard error. Titration curves with varying CF_3SO_2Na concentration for all peptides are shown in SI Figure S1.

FAP peptide. For the FAP peptide, an increase in CF_3SO_2Na **(**0.75 mM to 30 mM), resulted in a positive trend in •CF_3 labeling (0.7% to 11%), while •OH labeling exhibited a downward trend (89% to 37%) (SI Figure S1d). For the remaining 5 peptides, the lowest levels of •OH (0.2 - 37%) and •CF_3 labeling (<1 %) were observed at 30 mM CF_3SO_2Na concentration. In contrast, 0.75 mM of CF_3SO_2Na resulted in over-labeling (~50-92%) of all peptides by •OH, except for the Syn peptide (~4%), which contains all low •OH reactive AAs (SI Figure S1). The •CF_3-modified adducts at 0.75 mM of CF_3SO_2Na were measured to be at the lowest level for peptides containing AAs highly reactive to •CF_3 such as Trp (FAP, 0.7%), His (AG-II, 1.2%), and Phe in the short peptide (Met5, 0.2%). In comparison, the •CF_3-modified adducts at 0.75 mM of CF_3SO_2Na were at the highest level for peptides with the lowest •OH reactivity AAs (Syn, 17%), low to medium •OH reactivity AAs (Glu-Fib, 2%) and highest •OH reactivity AAs (Amyl-B, 0.3%).

In the above experiments, the highest CF_3SO_2Na (30 mM) concentration proved optimal only for •CF_3 labeling of the FAP peptide, where Trp, having the highest •CF_3 reactivity, exhibited the highest modification fraction (Table 1). The over-labeling of highly •OH reactive peptides (FAP, Met5 and Amyl-B) towards •OH was quenched at the highest CF_3SO_2Na concentration (30 mM). However, the highest CF_3SO_2Na concentration led to a significant reduction in •OH modification of peptides with low and low to moderate •OH reactive AAs (FAP, Met5 and Amyl-B), potentially rendering them undetectable in protein footprinting experiments. Overall, at this absorbed •OH amount, we observed an optimal CF_3SO_2Na concentration ranging between 2.5 and 7.5 mM, providing an adequate extent of •CF_3 labeling (~1-10%) and •OH labeling (1-50%) for all model peptides.

We further optimized the dual •CF_3/•OH chemistry with six model peptides by varying the absorbed •OH amount and using selected CF_3SO_2Na concentrations (2.5 and 7.5 mM). We adjusted the absorbed •OH amount up to ~14-folds by modifying the incident X-ray flux conditions of the 17-BM beamline using Al attenuations (X-ray dose) ranging from 508 µm thickness (3.9×10^{15} •OH radicals) to 25 µm thickness (53.9×10^{15} •OH radicals).[16] We quantified the extent of •CF_3 and •OH modifications for each peptide with nanoLC-MS/MS (Figure 2). We observed that •CF_3-modified adducts in all model peptides were measured at the lowest level (<1%) with low absorbed •OH amount (3.9×10^{15}) and then increased with a higher absorbed •OH amount. This positive trend in •CF_3-modified adducts with absorbed •OH amount was consistent for both 2.5 and 7.5 mM CF_3SO_2Na and across all model peptides (SI Figure S2). We noticed a significant increase in •CF_3-modified adducts (2 - 12%) at high absorbed •OH amount (32.2×10^{15} and 53.9×10^{15}) for all model peptides except for AG-II, where •CF_3 adducts were highest at a moderate absorbed •OH amount (18.6×10^{15}). The multifold increase in •CF_3-modified adducts (0.1% to 12%) with an increase in absorbed •OH amount was most significant for Syn peptide with the lowest •OH reactive AAs (SI Figure S2a). In contrast to •CF_3 labeling for the Syn peptide, we observed no significant change in •OH-modified adducts with an increase in absorbed •OH amount. Peptides with low to moderate •OH reactive AAs, Glu-Fib and AG-II, exhibited a significant increase in •OH-modified adducts with an increase in absorbed •OH amount (SI Figure S2b-c). In comparison, peptides with highly •OH reactive AAs (FAP, Met5 and Amyl-B) showed a decrease in •OH-modified adducts with an increase in absorbed •OH amount (SI Figure S2d-f), which could be due to the channeling of •OH towards generating •CF_3, as there was an increase in •CF_3 adducts. In summary, the beneficial effect of a higher absorbed •OH amount on multiplex TFM labeling was substantial for all six model peptides, and we conclude that a high absorbed •OH amount (32.2×10^{15} and 53.9×10^{15}) and low CF_3SO_2Na concentrations (2.5 - 7.5 mM) balances dual •CF_3/•OH chemistry in a "one-pot" reaction and will provide close to ideal conditions for •OH induced multiplex TFM labeling across the majority of peptide sequences in protein footprinting experiments.

Relative reactivity of residues across model peptides. In traditional HRPF labeling, proteins labeled with •OH are proteolyzed with proteases, and the resulting peptides are separated

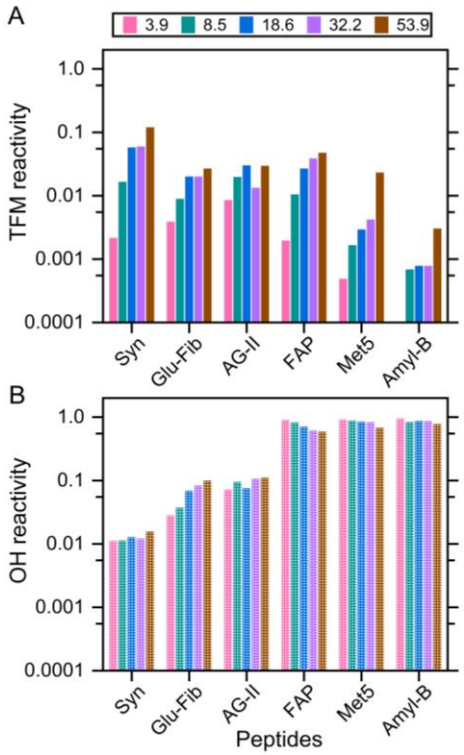

Figure 2. The dual •CF_3/•OH chemistry in multiplex TFM labeling was optimized with six model peptides by varying absorbed •OH amount and keeping a constant sodium triflinate concentration (2.5 mM CF_3SO_2Na). The modified fraction of (A) •CF_3 (solid bars) and (B) •OH (checkered bars) labeled peptides at varying absorbed •OH amount, was plotted on Log_{10} scale. Individual peptides were irradiated with X-rays for 20 ms and labeled at varying absorbed •OH amount by changing aluminum thickness attenuation, 508 µm (magenta), 305 µm (green), 152 µm (blue), 76 µm (purple) and 25 µm (brown) on 17-BM beamline. Titration curves with varying absorbed •OH amount for individual peptides at 2.5 mM and 7.5 mM CF_3SO_2Na concentrations are shown in SI Fig S2.

via reverse phase chromatography.[8, 17] Specific oxidation sites are then determined by tandem MS/MS analysis. To develop multiplex TFM labeling, we utilized a nanoLC-MS/MS setup identical to HRPF labeling workflows, facilitating an easier adaption for protein TFM footprinting experiments. We examined the dual •CF_3/•OH reactivity of AAs in all model peptides by quantifying their modifications (Table 1). The mass shifts of •CF_3 (+68 Da) and •OH (+14 Da, +16 Da) modifications were significant, and due to their opposite polarity, the •CF_3 and •OH-labeled isomers of modified peptides (e.g. Amyl-B) eluted separately on the reverse phase column (Figure 3a). •CF_3 modified isomers of different AAs in the Amyl-B peptide (isotopologues) were resolved, enabling their quantification at the single residue level, akin to •OH modified isomers (Figures 3b-c). Methionine (Met), with the highest •OH reactivity, typically dominates HRPF reactions, muting the reactivity of other proximal residues. This dominance is evident in HRPF labeling for Met peptides like Amyl-B (M1 + 16) and Met5 (M5 + 16), where the •OH-modified Met adduct (+ 16 Da) remains the highest modification (Amyl-B) or the only quantifiable product (Met5). In

Peptide	Sequence	HRPF OH k_{OH} / s^{-1}	Multiplex TFM-HRPF		
			k_{CF_3} / s^{-1}	k_{OH} / s^{-1}	CF_3:OH DR ratio
Syn	G**R**$^{\#}$G**D**T**P**	3.75 (0.19)	1.98 (0.07)	0.52 (0.08)	3.8:1
Glu-Fib	E**G**V**N**D**N**E E**G**F**F**S**A**R	6.03 (1.04)	2.13 (0.08)	7.52 (0.43)	1:3.5
AG-II	D*RV**Y**I**H**PF H**L**	7.04 (0.47)	2.67 (0.12)	4.62 (0.16)	1:1.7
FAP	**W**Q**P**P**R**A**R**I	18.32 (1.91)	4.93 (0.57)	26.57 (4.19)	1:5.4
Met5	**Y**G**G**F**M**	19.03 (1.46)	1.47 (0.14)	38.76 (4.83)	1:26.4
Amyl-B	M$^{\#}$**L**G**I**I**A**GK N**S**G	21.67 (1.66)	0.56 (0.05)	36.36 (3.53)	1:65

Table 1. The comparison of labeling efficiency for optimized multiplex TFM labeling against HRPF for six model peptides. The multiplex TFM labeling was done at 2.5 mM CF_3SO_2Na concentration and with 76 µm Al thickness (32.2×10^{15} •OH). The HRPF labeling was done at 0 mM CF_3SO_2Na concentration and with 864 µm Al thickness ($<1.8 \times 10^{15}$ •OH). Individual peptides were irradiated on 17-BM beamline and first order rate constants were calculated by fitting unmodified fraction of •CF_3 and •OH-modified peptides against X-ray exposure times (0 ms, 12 ms, 20 ms and 30 ms). Labeled AAs (bold) were colored as purple (detected in only multiplex TFM), blue (detected in both multiplex TFM and HRPF) and green (detected in only HRPF).

multiplex TFM labeling, we could quantify •CF_3 modifications for several AAs in Amyl-B (G3, A6, N9 and S10) and Met5 (Y1 and F4). Similar to Met-containing peptides, we observed additional •CF_3 labeled AAs (P3 and P4) in the FAP peptide with highly •OH reactive tryptophan (W1). Multiplex TFM labeling advantages extended to the low •OH reactive peptide, Syn (D4 and T5), low to moderate •OH reactive peptides, Glu-Fib (V3, N4, D5 and S12) and AG-II (D1), where •CF_3-modified adducts were detected for several AAs. The merit of dual •CF_3/•OH chemistry was evident through a complete overlap of •OH-modified adducts (23 AAs) in multiplex TFM and HRPF labeling experiments for all model peptides. Additionally, we detected both •CF_3 and •OH modified adducts for several AAs (14 AAs) in six model peptides, further increasing data rigor for footprinting analysis. Overall, we detected ~70% AAs (38/54) labeled in multiplex TFM labeling for all model peptides, representing a significant increase compared to ~43% of AAs (23/54) labeled in HRPF alone.

The balanced dynamic range ($k(CF_3)/k(OH)$) of dual •CF_3/•OH chemistry and the uniform labeling of AAs in •CF_3/•OH channels can help explain the robust efficiency of multiplex TFM labeling in model peptides. For the highly •OH reactive Amyl-B peptide, the dynamic range of •OH reactivity is 1000x for Met against Gly, making •OH modifications for Gly (0.0005 - 0.1%) outside the typical mass spectrometry detection range (10^4 - 10^5) relative to the most abundant ion.[18] The dynamic range of •CF_3/•OH reactivity over •OH reactivity for Amyl-B peptide was reduced ~10 times (~123) for non-optimized CF_3SO_2Na (30 mM) and further decreased ~2 times (~65) for optimized

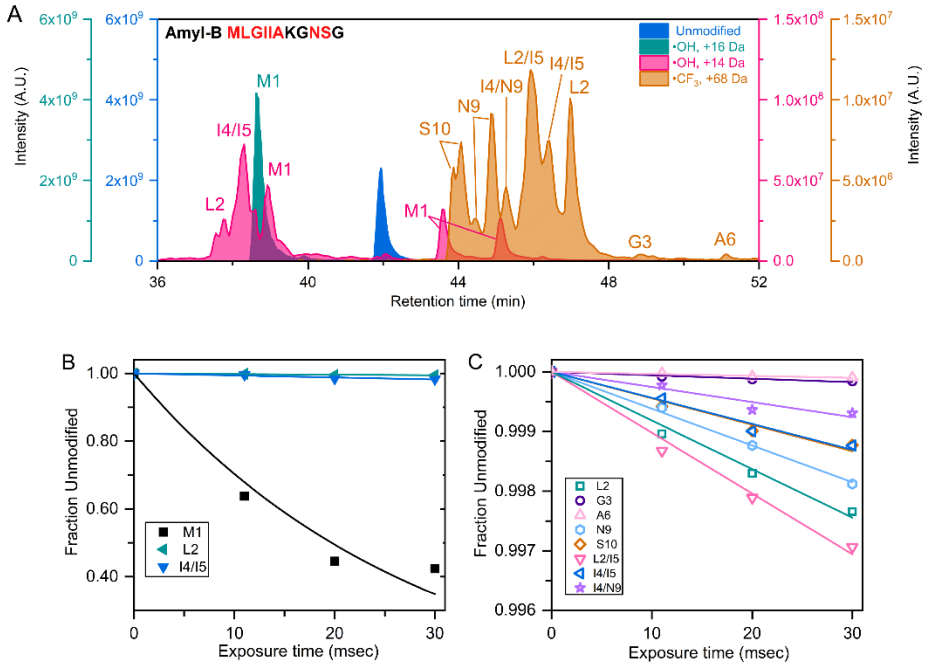

Figure 3. (a) The extracted ion chromatograph of •CF_3-labeled adducts (orange), •OH-labeled adducts (green and pink), and unmodified Amyl-B peptide is shown for multiplex TFM labeling experiment. (b) The unmodified fraction of •OH-labeled AAs and (c) •CF_3-labeled AAs in Amyl-B peptide was plotted against exposure time for multiplex TFM labeling experiment.

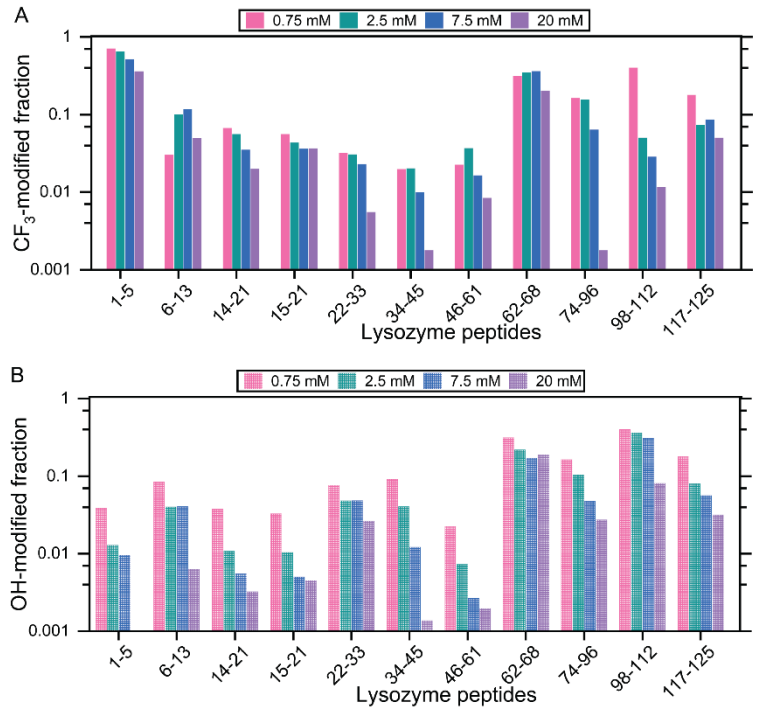

Figure 4. The dual •CF_3/•OH chemistry in multiplex TFM labeling was optimized with protein lysozyme by varying sodium triflinate (CF_3SO_2Na) concentration between 0.75 – 20 mM. The average modified fraction of (A) •CF_3 (solid bars) and (B) •OH (checkered bars) was plotted on Log_{10} scale for lysozyme peptides at different TFM reagent concentrations (magenta, green, blue and purple). Lysozyme samples with different CF_3SO_2Na concentrations were irradiated with X-rays for 20 ms at 76 µm Al thickness attenuation on 17-BM beamline.

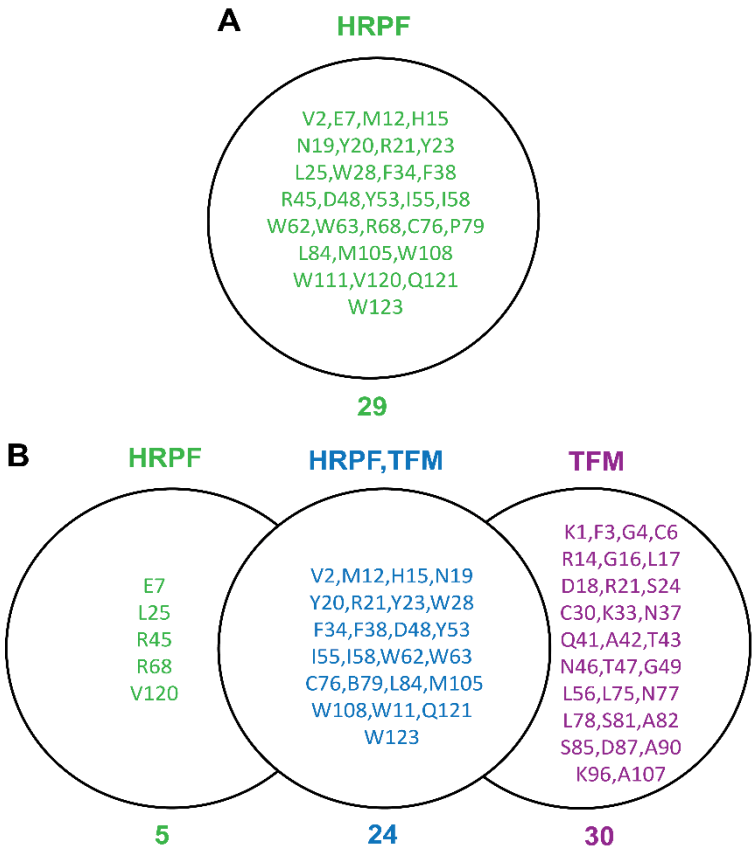

Figure 5. A comparison of lysozyme residues labeled in HRPF and Multiplex TFM labeling experiments. (A) Lysozyme residues labeled with •OH in HRPF alone. Lysozyme with 0 mM CF_3SO_2Na concentration was irradiated with X-rays for 20 ms at 864 µm Al thickness attenuation on 17-BM beamline. •OH-modified lysozyme residues in HRPF were colored green. (B) Venn diagram for lysozyme residues labeled in HRPF and optimized multiplex TFM labeling experiments. Lysozyme with 2.5 mM CF_3SO_2Na concentration and 32.2×10^{15} absorbed •OH amount was irradiated with X-rays for 20 ms at 76 µm Al thickness attenuation on 17-BM beamline. Labeled lysozyme residues in Venn diagram were colored as purple (detected in only multiplex TFM), blue (detected in both multiplex TFM and HRPF) and green (detected in only HRPF).

CF_3SO_2Na (2.5 mM) concentrations (Table 1 and SI Table S1). For the remaining five peptides, the dynamic range of $•CF_3$ reactivity was either higher than •OH reactivity for the low •OH reactive peptide (Syn) or more balanced for low to moderate •OH reactive peptides (Glu-Fib and AG-II) and highly •OH reactive peptides (FAP and Met5). Overall, the optimization of CF_3SO_2Na concentration improved the dynamic range of $•CF_3$/•OH reactivity to 2-7 fold and significantly increased peptide modification rates in both $•CF_3$ and •OH channels across all six model peptides. In addition to a balanced dynamic range, we observed uniform labeling of AAs in $•CF_3$ (28 AAs) and •OH (24 AAs) channels for all six model peptides in optimized multiplex TFM labeling relative to mono-labeling with •OH (23 AAs) in HRPF alone. The two-fold increase in the number of labeled AAs in multiplex TFM labeling relative to HRPF was evident with the labeling of AAs with the lowest •OH reactivity (Thr < Ser < Pro < Glu < Asn < Asp < Ala < Gly) in the $•CF_3$ channel or •OH channel (Glu) and the labeling of moderate •OH reactive AAs (Leu < Ile < Arg < Val) and highly •OH reactive AAs (Met < Trp < Tyr < Phe < His) in both $•CF_3$ and •OH channels. Two AAs, Lys (Amyl-B) and Gln (FAP) were not labeled in both multiplex TFM and HRPF labeling experiments, likely due to neighboring effects in peptides. The labeling of 17 AAs for six model peptides in multiplex TFM labeling coincided well with the dual $•CF_3$/•OH reactivity of 20 protein side chains in a competition-free environment.

Validation of optimized multiplex TFM labeling methods to enhance structural resolution for protein. The ~2-fold increase in the number of labeled AAs and the optimization of •OH induced multiplex TFM labeling with six model peptides established a baseline dataset for TFM protein footprinting. We assessed the robustness of multiplex TFM labeling for protein footprinting with hen egg white lysozyme (129 AAs, 14.3 kDa) by employing sodium triflinate (CF_3SO_2Na) as a TFM reagent and using synchrotron X-rays from the 17-BM beamline at NSLS-II for radiolysis. Trypsin digestion of lysozyme yielded 11 peptides with ~89% sequence coverage, and we quantified the extent of $•CF_3$ and •OH modifications for each lysozyme

peptide using nanoLC-MS/MS. To optimize multiplex TFM labeling for proteins, we exposed lysozyme (20 µM) with X-rays for 20 ms and tested various CF_3SO_2Na concentrations (0.75 mM, 2.5 mM, 7.5 mM and 20 mM), while maintaining a fixed absorbed •OH amount (32.2×10^{15}) with 76 µm Al thickness at the 17-BM X-ray footprinting beamline. The extent of both $•CF_3$ and •OH labeling for lysozyme peptides varied as a function of CF_3SO_2Na concentration (Figure 4). The high CF_3SO_2Na concentration (20 mM) caused a significant scavenging effect for both $•CF_3$ and •OH labeling chemistries for all lysozyme peptides, which is consistent with our model peptides study (Figure 4). The extent of $•CF_3$ labeling for lysozyme peptides was highest at 0.75 mM or 2.5 mM CF_3SO_2Na concentrations and then decreased significantly at a higher 7.5 mM CF_3SO_2Na concentration. The highest level of •OH-modified products across all lysozyme peptides was observed at the lowest CF_3SO_2Na concentration (0.75 mM) followed by a decrease at higher CF_3SO_2Na concentrations. In summary, the high absorbed •OH amount (32.2×10^{15}), and low CF_3SO_2Na concentrations (0.75 – 2.5 mM) balanced dual $•CF_3$/•OH chemistry in a "one-pot" reaction and would provide ideal conditions for •OH induced multiplex TFM labeling across lysozyme peptides.

We then examined the dual $•CF_3$/•OH reactivity of lysozyme by comparing the labeling efficiency in optimized multiplex TFM labeling (2.5 mM CF_3SO_2Na and 32.2×10^{15} •OH) with non-optimized multiplex TFM labeling (20 mM CF_3SO_2Na and 8.5×10^{15} •OH) and HRPF labeling (0 mM CF_3SO_2Na). We detected a 1.9-fold enhancement in optimized multiplex TFM labeling for lysozyme with 54 labeled residues, compared to 29 residues in HRPF (Figure 5). The optimization of TFM conditions significantly enhanced multiplex labeling to 54 residues as only 26 residues were labeled in $•CF_3$/•OH channels for non-optimized conditions (SI Figure S3). Overall, we detected a significant enhancement of structural resolution in lysozyme with ~47% of residues (54/115) labeled in optimized multiplex labeling, compared to ~25% of residues (29/115) in HRPF alone. Further, the number of labeled residues per peptide were ranging from 22 to 88 % across 11 lysozyme peptides in multiplex labeling, with the average value per peptide of 50 % (SI Table S3).

Similar to model peptides, the robust efficiency of multiplex TFM labeling in lysozyme could be attributed to a balanced dynamic range of dual $•CF_3$/•OH chemistry and the uniform labeling of residues in $•CF_3$/•OH channels. Similar to the model peptides, the most efficient labeling in $•CF_3$/•OH channels was observed for peptides containing low to moderate •OH reactive residues (1-5, 14-21, 15-21, 34-45, 46-61 and 74-96) and highly •OH reactive residues (6-13, 22-33, 62-68 and 117-125) compared to that for HRPF alone (Table S2). Moreover, the propensity of labeling of lysozyme residues with the lowest •OH reactivity (e.g. Thr43, Ser24, Pro79, Gln41, Asn37, Asp18, Ala42, Gly4) was significantly higher in multiplex TFM labeling relative to HRPF alone. Lysozyme residues with moderate and high •OH reactivity were either detected only in multiplex TFM labeling (Cys6, Phe3, Leu17, Lys33) or overlapped with HRPF labeling (Cys76, Met12, Trp28, Tyr20, Phe34, His15, Leu84, Ile55, Arg21, Val2). Similar to Met-containing model peptides, we detected $•CF_3$ modifications for additional residues in Met-containing lysozyme peptides, 6-13 (Cys6) and 98-112 (Ala107, Trp108). In summary, the multiplex TFM labeling for lysozyme was efficient in dual $•CF_3$/•OH channels and followed trends observed in model peptides.

Range	Lysozyme peptides	HRPF OH Fraction Unmod.	Multiplex TFM-HRPF	
			CF_3 Fraction Unmod.	OH Fraction Unmod.
1-5	K V# F G R 94 88 12 39 67	0.9875	0.3431	0.9870
6-13	C E L A A A M K 48 81 0 0 38 23 2 72	0.9520	0.8983	0.9591
14-21	R H G L D* N Y R 175 36 36 0 38 81 67 115	0.9414	0.9434	0.9891
15-21	H G L D N# Y# R 36 36 0 38 81 67 115	0.9621	0.9559	0.9895
22-33	G Y S L G N W V C A A K* 46 46 35 3 0 19 0 0 0 0 0 58	0.9662	0.9688	0.9510
34-45	F E S N F N T Q A T N R 48 17 8 83 15 40 1 108 21 46 86 89	0.9495	0.9794	0.9589
46-61	N T D G S T D Y G I L* Q I 52 126 62 24 1 6 26 18 0 3 1 5 3 N S R 30 0 89	0.9833	0.9626	0.9926
62-68	W W# C N D G R 123 46 0 56 21 33 111	0.9553	0.6475	0.7784
74-96	N L* C# N I* P C S A L L S 34 81 7 108 47 78 0 69 28 1 36 60 S D I T A S V N C A K* 57 87 7 57 23 1 1 73 3 0 47	0.8418	0.8433	0.8941
98-112	I V S D G N G M N A W 7 0 24 48 35 99 13 0 43 28 11 V A W R 94 11 12 90	0.6289	0.9491	0.6325
117-125	G T D V Q A W I R 45 67 86 14 109 30 55 34 151	0.9360	0.9260	0.9185

Table 2. The comparison of labeling efficiency for optimized multiplex TFM labeling against HRPF for six model peptides. The multiplex TFM labeling was done at 2.5 mM CF_3SO_2Na concentration and with 76 µm Al thickness (32.2×10^{15} •OH). The HRPF labeling was done at 0 mM CF_3SO_2Na concentration and with 864 µm Al thickness ($<1.8 \times 10^{15}$ •OH). Individual peptides were irradiated on 17-BM beamline and first order rate constants were calculated by fitting unmodified fraction of $•CF_3$ and •OH-modified peptides against X-ray exposure times. Labeled AAs (bold) were colored as purple (detected in only multiplex TFM), blue (detected in both multiplex TFM and HRPF) and green (detected in only HRPF).

In a protein environment, solvent accessibility is another criterion for •OH modifications in addition to the intrinsic reactivity of protein side chains. We analyzed whether $•CF_3$ labeling also correlates with the solvent accessibility of lysozyme residues (Table 2). Theoretical measures of solvent accessibility (SASA) for all residues in lysozyme sequence were calculated using the VADAR algorithm and the lysozyme crystal structure (PDB: 6LYZ).[19-20] We determined that residues accessible to the solvent were labeled with $•CF_3$ radicals across the lysozyme protein structure. For example, highly solvent-accessible D18 (38 Å^2), D48 (62 Å^2), and D87 (87 Å^2) were all labeled with $•CF_3$, while low solvent-accessible D52 (26 Å^2) and D66 (21 Å^2) were not. On the other hand, we were unable to observe the modification of solvent-accessible D101 (48 Å^2) and D119 (86 Å^2) due to the presence of the most $•CF_3$ reactive Trp residue in peptides 98-112 and 117-125. Similarly, solvent-accessible Q41 (108 Å^2) was $•CF_3$-labeled, while low solvent-accessible Q57 (5 Å^2) was unlabeled. On the other hand, solvent-accessible Q121 (108 Å^2) remained unmodified by $•CF_3$ due to its location in the peptide 117-125, containing the most $•CF_3$ reactive Trp residue. Lastly, peptide 74-96 consists of N74 (34 Å^2), N77 (108 Å^2), N93 (73 Å^2), S81 (69 Å^2), S85 (60 Å^2), S86 (57 Å^2) and S91 (1

Å^2) residues, of which residues most accessible to bulk solvent, including N77, S81, S85, and S86 were labeled, while residues less accessible to the solvent, including N74, N93 and S91 were not. Out of the 20 protein side chains in lysozyme, only glutamic acid was not labeled in multiplex TFM labeling either due to adjacent highly •CF_3 reactive (Cys6) and highly •OH reactive (Met11) residues in segment 6-13 (Glu7) or low solvent accessibility in segment 34-45 (Glu35, 17 Å^2 SASA). The occurrence of highly •CF_3 reactive and solvent accessible, Tryptophan, (62-68, 98-112, 117-125) attenuated the multiplex labeling of other residues in these segments. However, Trp residues present the lowest abundance of the 20 naturally occurring AAs in proteins and Trp frequency is of only a 1.4% in comparison to 4.7% frequency in lysozyme.[21] Hence, high •CF_3 reactivity of Trp residues will not be a detrimental factor for protein TFM footprinting.

CONCLUSIONS

We found •CF_3 as a protein footprinting probe to be quite complementary to •OH in multiplex TFM labeling experiment. The mass shifts for •CF_3 modifications are distinct from all major known •OH modifications, and the retention times of •CF_3-modified peptides are more hydrophobic than the unmodified peptides. Thus, •CF_3-modified peptides do not make the LC-MS chromatograph especially complex or overlap with most •OH-modified peptides. We detected the labeling of additional new protein side chains in multiplex TFM labeling, and there was an overlap of protein side chains labeled in •CF_3/•OH channels against •OH labeling in HRPF. Several protein side chains were labeled in both •CF_3/•OH channels in multiplex TFM labeling, increasing data rigor. We observed protein side chains that are refractory to HRPF labeling, such as Thr < Ser < Pro < Glu < Gln < Asn < Asp < Ala < Gly, were modified with •CF_3 in multiplex TFM labeling. In addition, Met shows low reactivity to •CF_3 in multiplex TFM chemistry, which allows detection and quantification of additional protein side chains labeled by •CF_3 across Met containing peptides. We can now employ optimized multiplex TFM workflow to target all 20 protein side chains in •CF_3/•OH channels using a single TFM reagent.

The •OH can also be generated through other platforms such as gamma rays, electron beams, electric discharge or a plasma source, decomposition of hydrogen peroxide using transition metal-based Fenton chemistry, and photolysis of hydrogen peroxide using lasers (FPOP) or a high-pressure flash oxidation lamp.[22-27] The successful development of the multiplex TFM labeling with XFP will motivate its implementation on other •OH generating platforms. This broad implementation will increase accessibility of the multiplex TFM labeling for addressing structural biology questions and accelerating higher order structural analysis for biopharmaceutical development.

METHODS

Materials. TFM reagent sodium triflinate (CF_3SO_2Na, ≥95% purity), Lysozyme from chicken egg white (≥98% purity) and Methionine amide were purchased from Millipore Sigma. Model peptides (Glu-Fib, AG-II, FAP, Met5 and Amyl-B) were purchased from Millipore Sigma. BACHEM Synthetic peptide was purchased from BACHEM and also synthesized from GenScript. Alexa Fluor™ 488 NHS Ester and 10× PBS solution were purchased from Fisher Scientific. HPLC-grade Acetonitrile and HPLC-grade water were purchased from Honeywell-Burdick & Jackson.

TFM and HRPF labeling of model peptides and lysozyme. X-ray exposure of samples was carried out at the X-ray Footprinting of Biological Materials (XFP) beamline located at the National Synchrotron Light Source II (NSLS-II, Brookhaven National Laboratory, Upton, NY), using a 96-well high-throughput apparatus at a constant temperature of 25 °C and ring current of 400 mA.[16] Incident beam powers on the samples as a function of attenuation were determined as described previously.[11] Samples were exposed in 5 µL volumes in 200 µL PCR tubes, with 8 replicates for each sample and exposure condition.

The working solutions for model peptides were prepared at 60 µM concentration with 1×PBS (pH 7.4) for labeling experiments. 20 µM model peptides with 1×PBS, in varying CF_3SO_2Na concentrations (0.25 mM, 0.75 mM, 2.5 mM, 7.5 mM and 30 mM) and varying absorbed •OH amount by changing aluminum thickness attenuation (508 µm, 305 µm, 152 µm, 76 µm and 25 µm), were X-ray exposed individually for 20 ms to optimize TFM labeling conditions. X-ray exposures for optimized TFM labeling conditions (2.5 mM CF_3SO_2Na, 76 µm aluminum thickness) in model peptides were performed independently at multiple exposure times of 0 ms, 12 ms, 20 ms, and 30 ms to calculate the rate constants in dose-response studies. X-ray exposures for HRPF labeling (0 mM CF_3SO_2Na, 762 µm aluminum thickness) in model peptides were performed independently at multiple exposure times of 0 ms, 12 ms, 20 ms, and 40 ms to calculate the rate constants in dose-response studies. The working Lysozyme solution at 100 µM (1.4 mg/ml) concentration was reconstituted with 1×PBS (pH 7.4) for labeling experiments. 20 µM Lysozyme samples, in varying CF_3SO_2Na concentrations (0.75 mM, 2.5 mM, 7.5 mM and 20 mM), were X-ray exposed for 20 ms with 76 µm aluminum thickness. 20 µM Lysozyme samples for hydroxyl labeling (0 mM CF_3SO_2Na) were X-ray exposed for 20 ms with 864 µm aluminum thickness.

Labeled samples were immediately mixed with 60 mM methionine amide solution (1.1 µl) to a final concentration of ~11 mM methionine amide to quench secondary radicals. Quenched samples were frozen in liquid nitrogen and shipped on dry ice to CWRU for mass spectrometric analysis.

Mass spectrometry sample preparation and chromatography separation. The frozen labeled samples from -80 °C were first thawed on ice. Lysozyme samples (2.8 µg in 10 µL) were dried completely via speed-vacuum and reconstituted in 20 mM Tris / 6 M urea buffer (pH 8.0). They were then reduced with 10 mM dithiothreitol (DTT) at 37 °C for 45 min followed by alkylation with 25 mM iodoacetamide at room temperature for 1 hour in the dark. Lysozyme samples were then digested with trypsin at 37 °C overnight using a 1:10 enzyme to protein molar ratio. The digestion reaction was terminated by adding 5% formic acid to a final concentration of 0.1%.

Model peptides and digested lysozyme samples were diluted with 0.1% formic acid and analyzed by a Waters nanoACQUITY UPLC coupled to a Thermo Orbitrap™ Eclipse Tribrid mass spectrometer. They were desalted and concentrated using a Waters nanoACQUITY UPLC C_{18} trap column (100 Å, 5 µm, 180 µm × 20 mm) and eluted from a Waters ACQUITY UPLC BEH C_{18} analytical column (300 Å, 1.7 µm, 75 µm × 250 mm). Two mobile phase systems - mobile phase A (0.1% FA in water) and mobile phase B (0.1% FA in Acetonitrile) were utilized for separation using a LC gradient, Syn (0% to 32% B), Glu-Fib (0% to 40% B), AG-II (0% to 50% B), FAP (0% to 40% B), Met5 (0% to 32% B), Amyl-B (0% to 45% B) and lysozyme (0% to 32% B) for 62 min at a flowrate of 300 nL/min and the capillary voltage of 2.1 kV. The gradient was then increased to 70% B from 62 to 66 min to allow the complete elution of peptides from the analytical column. The C_{18} column was then washed with 98% B and re-equilibrated with 0% B solvent for 10 and 14 min respectively. Analytical column temperature was maintained at 40 °C.

Mass spectrometry data collection and analysis. Full mass spectra were acquired in a positive polarity and the Orbitrap resolution was set to 120,000, an RF lens setting of 30 with an AGC target of 4×10^5 ions and maximum injection time was 50 ms. Precursor ions were chosen in a DDA mode followed by MS/MS fragmentation by CID with the collision energy set at 35% with an AGC target of 10,000 ions and IonTrap detection of fragment ions. MassMatrix Xtreme (v3.0.10.25, MassMatrix) was used to search for unmodified and •OH/•CF_3 labeled peptides (variable •OH/•CF_3 modifications, no fixed modifications) against the database containing model peptides and lysozyme protein. Peptides were searched with a maximum of one missed cleavage, ±10.00 ppm peptide mass tolerance and ±0.80 Da (CID) fragment mass tolerance. Xcalibur software was used for manually extracting chromatograms and analyzing the modification of peptides based on MassMatrix Xtreme output. OriginLab software was used to plot dose-response curve and calculate the modification rate for each modified peptide.

ASSOCIATED CONTENT

Supporting Information

Multiplex TFM labeling was optimized with six model peptides by varying TFM reagent concentration and keeping a constant absorbed •OH amount (Figure S1, S-2), multiplex TFM labeling was optimized with six model peptides by varying absorbed •OH amount (Figure S2, S-3), Venn diagram to compare lysozyme residues labeled in HRPF and non-optimized multiplex TFM labeling experiments (Figure S3, S-4), The comparison of labeling efficiency for non-optimized multiplex TFM labeling against HRPF for six model peptides (Table S1, S-5). The comparison of reactivity coverage for optimized multiplex TFM labeling against HRPF for lysozyme (Table S2, S-6).

The Supporting Information is available free of charge on the ACS Publications website.

SI Optimized Trifluoromethylation and OH Radical Labeling with Radiolysis (PDF)

AUTHOR INFORMATION

Corresponding Author

*__Janna Kiselar__ - Center for Proteomics and Bioinformatics; Department of Nutrition, Case Western Reserve University, School of Medicine, 10900 Euclid Avenue, Cleveland, Ohio 44106, USA.
*Email: jxk217@case.edu

Authors

__Rohit Jain__ - Center for Synchrotron Biosciences; Center for Proteomics and Bioinformatics; Department of Nutrition, Case Western Reserve University, School of Medicine, 10900 Euclid Avenue, Cleveland, Ohio 44106, USA.
__Erik R. Farquhar__ – - Center for Synchrotron Biosciences; Department of Nutrition, Case Western Reserve University, School of Medicine, 10900 Euclid Avenue, Cleveland, Ohio 44106, USA.
__Nanak S. Dhillon__ – Department of Nutrition, Case Western Reserve University, School of Medicine, 10900 Euclid Avenue, Cleveland, Ohio 44106, USA.
__Mark R. Chance__ - Center for Synchrotron Biosciences; Center for Proteomics and Bioinformatics; Department of Nutrition, Case Western Reserve University, School of Medicine, 10900 Euclid Avenue, Cleveland, Ohio 44106, USA.

Author Contributions

R.J., E.F., N.S.D. and N.J. prepared samples and performed experiments. R.J. and J.K. designed experiments, analyzed data, and wrote the manuscript. E.F. and M.R.C. contributed to editing the manuscript. All authors have given approval to the final version of the manuscript.

Conflict of interest statement

The authors declare the following financial interests/personal relationships which may be considered as potential competing interests. M.R.C. is a Founder and Chief Scientific Officer of NeoProteomics, which provides access to footprinting technologies and services. J.K. is a consultant for NeoProteomics. M.R.C. owns shares and is a member of the scientific advisory board of GenNext® Technologies, Inc., makers of the benchtop flash oxidation system.

ACKNOWLEDGMENT

This research was supported by NIH R01 grant number GM141078. Funding for development of the XFP beamline was provided by a Major Research Instrumentation award from the NSF (DBI-1228549) and Case Western Reserve University. This research used resources of the NSLS-II, a U.S. DOE Office of Science User Facility operated for the DOE Office of Science by Brookhaven National Laboratory under Contract No. DE-SC0012704. The DOE has established a portal for accessing X-ray footprinting beamlines at: https://berstructuralbioportal.org/x-ray-footprinting/

REFERENCES

1. Chance, M. R.; Farquhar, E. R.; Yang, S.; Lodowski, D. T.; Kiselar, J., Protein Footprinting: Auxiliary Engine to Power the Structural Biology Revolution. *Journal of molecular biology* **2020,** *432* (9), 2973-2984.
2. Jain, R.; Muneeruddin, K.; Anderson, J.; Harms, M. J.; Shaffer, S. A.; Matthews, C. R., A conserved folding nucleus sculpts the free energy landscape of bacterial and archaeal orthologs from a divergent TIM barrel family. *Proceedings of the National Academy of Sciences of the United States of America* **2021,** *118* (17).

3. Liu, X. R.; Zhang, M. M.; Gross, M. L., Mass Spectrometry-Based Protein Footprinting for Higher-Order Structure Analysis: Fundamentals and Applications. *Chemical reviews* **2020,** *120* (10), 4355-4454.
4. Vierstra, J.; Stamatoyannopoulos, J. A., Genomic footprinting. *Nature methods* **2016,** *13* (3), 213-21.
5. Adilakshmi, T.; Soper, S. F.; Woodson, S. A., Structural analysis of RNA in living cells by in vivo synchrotron X-ray footprinting. *Methods in enzymology* **2009,** *468*, 239-58.
6. Dominguez-Martin, M. A.; Hammel, M.; Gupta, S.; Lechno-Yossef, S.; Sutter, M.; Rosenberg, D. J.; Chen, Y.; Petzold, C. J.; Ralston, C. Y.; Polívka, T.; Kerfeld, C. A., Structural analysis of a new carotenoid-binding protein: the C-terminal domain homolog of the OCP. *Scientific reports* **2020,** *10* (1), 15564.
7. Maleknia, S. D.; Brenowitz, M.; Chance, M. R., Millisecond Radiolytic Modification of Peptides by Synchrotron X-rays Identified by Mass Spectrometry. *Analytical chemistry* **1999,** *71* (18), 3965-3973.
8. Kiselar, J.; Chance, M. R., High-Resolution Hydroxyl Radical Protein Footprinting: Biophysics Tool for Drug Discovery. *Annual review of biophysics* **2018**.
9. Huang, W.; Ravikumar, K. M.; Chance, M. R.; Yang, S., Quantitative mapping of protein structure by hydroxyl radical footprinting-mediated structural mass spectrometry: a protection factor analysis. *Biophys J* **2015,** *108* (1), 107-15.
10. Xu, G.; Chance, M. R., Hydroxyl radical-mediated modification of proteins as probes for structural proteomics. *Chemical reviews* **2007,** *107* (8), 3514-43.
11. Jain, R.; Dhillon, N. S.; Farquhar, E. R.; Wang, B.; Li, X.; Kiselar, J.; Chance, M. R., Multiplex Chemical Labeling of Amino Acids for Protein Footprinting Structure Assessment. *Analytical chemistry* **2022,** *94* (27), 9819-9825.
12. Zhang, H.; Wen, J.; Huang, R. Y.; Blankenship, R. E.; Gross, M. L., Mass spectrometry-based carboxyl footprinting of proteins: method evaluation. *International journal of mass spectrometry* **2012,** *312*, 78-86.
13. Cheng, M.; Zhang, B.; Cui, W.; Gross, M. L., Laser-Initiated Radical Trifluoromethylation of Peptides and Proteins: Application to Mass-Spectrometry-Based Protein Footprinting. *Angewandte Chemie (International ed. in English)* **2017,** *56* (45), 14007-14010.
14. Cheng, M.; Asuru, A.; Kiselar, J.; Mathai, G.; Chance, M. R.; Gross, M. L., Fast Protein Footprinting by X-ray Mediated Radical Trifluoromethylation. *Journal of the American Society for Mass Spectrometry* **2020,** *31* (5), 1019-1024.
15. Meng, H.; Kumar, K., Antimicrobial activity and protease stability of peptides containing fluorinated amino acids. *Journal of the American Chemical Society* **2007,** *129* (50), 15615-22.
16. Jain, R.; Abel, D.; Rakitin, M.; Sullivan, M.; Lodowski, D. T.; Chance, M. R.; Farquhar, E. R., New high-throughput endstation to accelerate the experimental optimization pipeline for synchrotron X-ray footprinting. *Journal of synchrotron radiation* **2021,** *28* (Pt 5), 1321-1332.
17. Liu, X. R.; Rempel, D. L.; Gross, M. L., Protein higher-order-structure determination by fast photochemical oxidation of proteins and mass spectrometry analysis. *Nature Protocols* **2020,** *15* (12), 3942-3970.
18. Kaur, P.; Kiselar, J.; Yang, S.; Chance, M. R., Quantitative protein topography analysis and high-resolution structure prediction using hydroxyl radical labeling and tandem-ion mass spectrometry (MS). *Molecular & cellular proteomics : MCP* **2015,** *14* (4), 1159-68.
19. Diamond, R., Real-space refinement of the structure of hen egg-white lysozyme. *Journal of molecular biology* **1974,** *82* (3), 371-391.
20. Willard, L.; Ranjan, A.; Zhang, H.; Monzavi, H.; Boyko, R. F.; Sykes, B. D.; Wishart, D. S., VADAR: a web server for quantitative evaluation of protein structure quality. *Nucleic Acids Res* **2003,** *31* (13), 3316-9.
21. Santiveri, C. M.; Jiménez, M. A., Tryptophan residues: Scarce in proteins but strong stabilizers of β-hairpin peptides. *Peptide Science* **2010,** *94* (6), 779-790.
22. Minkoff, B. B.; Blatz, J. M.; Choudhury, F. A.; Benjamin, D.; Shohet, J. L.; Sussman, M. R., Plasma-Generated OH Radical Production for Analyzing Three-Dimensional Structure in Protein Therapeutics. *Scientific reports* **2017,** *7* (1), 12946.
23. Sharp, J. S.; Chea, E. E.; Misra, S. K.; Orlando, R.; Popov, M.; Egan, R. W.; Holman, D.; Weinberger, S. R., Flash Oxidation (FOX) System: A Novel Laser-Free Fast Photochemical Oxidation Protein Footprinting Platform. *Journal of the American Society for Mass Spectrometry* **2021,** *32* (7), 1601-1609.
24. Rosi, M.; Russell, B.; Kristensen, L. G.; Farquhar, E. R.; Jain, R.; Abel, D.; Sullivan, M.; Costello, S. M.; Dominguez-Martin, M. A.; Chen, Y.; Marqusee, S.; Petzold, C. J.; Kerfeld, C. A.; DePonte, D. P.; Farahmand, F.; Gupta, S.; Ralston, C. Y., An automated liquid jet for fluorescence dosimetry and microsecond radiolytic labeling of proteins. *Communications biology* **2022,** *5* (1), 866.
25. Li, K. S.; Shi, L.; Gross, M. L., Mass Spectrometry-Based Fast Photochemical Oxidation of Proteins (FPOP) for Higher Order Structure Characterization. *Accounts of chemical research* **2018,** *51* (3), 736-744.
26. Farquhar, E. R.; Vijayalakshmi, K.; Jain, R.; Wang, B.; Kiselar, J.; Chance, M. R., Intact mass spectrometry screening to optimize hydroxyl radical dose for protein footprinting. *Biochemical and Biophysical Research Communications* **2023,** *671*, 343-349.
27. Jain, R.; Dhillon, N. S.; Kanchustambham, V. L.; Lodowski, D. T.; Farquhar, E. R.; Kiselar, J.; Chance, M. R., Evaluating Mass Spectrometry-Based Hydroxyl Radical Protein Footprinting of a Benchtop Flash Oxidation System against a Synchrotron X-ray Beamline. *Journal of the American Society for Mass Spectrometry* **2024**.